Vol. 297: 71–81, 2005 | MARINE ECOLOGY PROGRESS SERIES
Mar Ecol Prog Ser | Published August 1

Deep chlorophyll *a* maxima (DCMs) in pelagic Antarctic waters. II. Relation to bathymetric features and dissolved iron concentrations

O. Holm-Hansen*, M. Kahru, C. D. Hewes

Scripps Institution of Oceanography, University of California-San Diego, La Jolla, California 92093-0202, USA

ABSTRACT: A deep chlorophyll *a* maximum (DCM) at depths between 60 and 90 m in waters south of the Antarctic Polar Front (APF) occurs only in pelagic waters where the chlorophyll *a* concentrations in the upper mixed layer (UML) are very low (generally <0.2 mg m^{-3}). Dissolved Fe concentrations in these waters with DCMs are also very low (generally <0.2 nM) and are probably a limiting factor for phytoplankton growth and biomass. DCMs occur in the upper portion of the temperature minimum layer (TML), which is the winter residue of the Antarctic Surface Water (AASW). The higher phytoplankton biomass at these depths is thought to result from higher Fe concentrations in the winter remnant of the AASW as compared to that found in the overlying UML. A survey of the literature indicates that DCMs are located predominately over the deep ocean basins where enrichment of surface waters with Fe from either coastal sediments or from upwelling processes would be minimal. DCMs are not found in coastal waters or in pelagic regions where complex bottom topography causes upwelling of deep water with sufficiently high Fe concentrations to enhance surface chlorophyll *a* concentrations. Such enrichment of surface waters overlying or downstream of topographical seamounts or ridges that rise to within a few thousand meters of the surface usually results in elevated phytoplankton biomass in the UML and no DCM due to decreased solar irradiance in the TML. The effect of such enrichment of Fe in surface pelagic waters that results from upwelling processes is most pronounced in the Scotia Sea, in the Polar Frontal region downstream of South Georgia, over the Southwest Indian Ridge, over the Kerguelen Plateau, and over the Pacific Antarctic and Southeast Indian Ridges.

KEY WORDS: Chlorophyll *a* · Deep chlorophyll *a* maxima · Southern Ocean · Iron · Bathymetry

INTRODUCTION

During the past 14 yr of the US Antarctic Marine Living Resources program in the southwestern Atlantic Ocean we have documented the annual occurrence of a deep chlorophyll *a* maximum (DCM) at depths between 60 and 90 m in Drake Passage waters to the northwest of Elephant Island. The chlorophyll *a* (chl *a*) concentrations in the upper mixed layer (UML, ~45 m) at these stations are low (~0.05 to 0.15 mg m^{-3}) compared to the higher concentrations (~0.2 to >1.0 mg m^{-3}) found at 60 to 90 m. All other stations in the sampling grid had maximal chl *a* concentrations in the UML and no DCM (Fig. 1). In a previous paper, Holm-Hansen & Hewes (2004) analyzed the occurrence of these DCMs in regard to physical, chemical, and optical conditions in the upper water column and concluded that the increase in phytoplankton biomass in these DCMs is the result of active phytoplankton growth occurring on a nutricline (most likely increasing Fe concentrations) within the temperature minimum layer (TML), which is the winter remnant of Antarctic Surface Water (AASW). This conclusion was supported both by direct measurement of photosynthetic rates in samples from the DCM in on-deck incubations with radiocarbon and also by measurement of

*Email: oholmhansen@ucsd.edu

cellular fluorescence at 683 nm with a passive fluorometer, which can be equated to instantaneous *in situ* photosynthetic rates (Kiefer et al. 1989, Chamberlin et al. 1990).

Low chl *a* concentrations in Antarctic pelagic waters that have excess major inorganic nutrients (Chisholm & Morel 1991) can be most easily ascribed to limiting concentrations of Fe (e.g. Martin et al. 1991, Boyd et al. 2000). As all our work with DCMs has been done in the southwestern Atlantic Ocean, it was of interest to see if such DCMs occur throughout the Southern Ocean (defined here as all waters south of the Polar Front) as an indicator of regions where Fe availability limits phytoplankton biomass. From an extensive literature review, we have cited the papers and the locations where DCMs have been reported and also papers reporting dissolved Fe concentrations at or close to those stations with DCMs. Concentrations of chl *a* and dissolved Fe in the UML of Antarctic waters are discussed with respect to the general circulation patterns of the Southern Ocean, as well as the influence of bottom topography, which might enrich surface waters with Fe originating from deep water or from bottom sediments.

OCCURRENCE AND SIGNIFICANCE OF A DCM

Surface chl *a* concentrations and location of DCMs in the Southern Ocean

After an extensive search of the literature relating to phytoplankton distributions in the Southern Ocean, the station locations where chl *a* profiles showed the presence of a DCM were found to be clustered in 3 main areas: (1) southeastern Pacific Ocean, Drake Passage, and southwestern Scotia Sea; (2) southern Indian Ocean; and (3) southern Australasian–Pacific sector. The locations of these stations are shown in Fig. 2A, which also shows the spatial distributions of chl *a* concentrations in surface waters during January and February 2000, as derived from satellite SeaWiFS data, as well as major bathymetric features (thin black lines). Fig. 2B shows the locations and names of the oceanic regions and bathymetric features mentioned throughout our paper. The clustering of DCM stations within these 3 areas is most likely the result of various national research cruises being concentrated in these regions. It should be noted that all stations having a DCM are located in low chl *a* waters. A few stations are located close to or within waters having slightly elevated chl *a* concentrations, but this is most likely the result of interannual variability in the distribution of chl *a* in the upper water column. It should be noted that the actual number of stations showing the presence of a DCM far exceeds the number of locations shown in Fig. 2. Many of the papers cited in Table 1 as showing the occurrence of a DCM are represented by only one symbol in Fig. 2, but actually report 2 to 3 locations in that general area where a DCM was evident. A few of the papers report DCMs at >17 different locations (Garibotti et al. 2003, Holm-Hansen et al. 2004). The AMLR program, although shown as only one symbol in Fig. 2, has annually documented between 15 and 40 locations with a DCM over the past 15 yr. There have been relatively few investigations of chl *a* concentrations with depth in large areas of the Southern Ocean with very low chl *a* in surface waters (e.g. the southern Pacific Ocean from 70 to 130° W and to the south of Africa from about 20° E to 20° W, 57 to 60° S), where the development of DCMs should be most pronounced. No DCMs have been found in waters where the chl *a* concentration in surface waters exceeds ~1.0 mg m^{-3} (Fig. 2).

Origin and characteristics of DCMs

Chl *a* maxima at depths <40 m in Antarctic waters are generally attributed to photoinhibition effects (Holm-Hansen et al. 1993, Smith & Cullen 1995); rare depletion of a major inorganic nutrient, such as nitrogen (e.g. Nelson & Smith 1986, Holm-Hansen et al. 1989); or to zooplankton grazing in surface waters. The formation of DCMs at depths >50 m is generally attributed to either (1) a nutrient limitation, where the chl *a* maximum develops at the depth of the nutricline for the limiting element, or (2) the settling of phytoplankton to deeper waters, which may happen after the occurrence of rich phytoplankton blooms in surface waters (Mikaelyan & Belyaeva 1995, Berdalet et al. 1997). Examination of all available data relating to the DCMs, as shown in Figs. 1 & 2, indicates that the following relationships apply to the occurrence of a DCM and the physical, chemical, and optical conditions in the upper water column:

(1) The depth of the chl *a* maximum is below the UML, as seen in Fig. 1B.

(2) The depth of the DCM is located within the TML, which is the winter remnant of the AASW. The TML tends to deepen from south to north, as does the depth of the DCM (Fiala et al. 1998, DiTullio et al. 2003).

(3) If chl *a* concentrations are moderately high (greater than ~0.8 mg m^{-3}) in the UML, there is generally no DCM in the TML (Fig. 1C).

(4) Concentrations of essential macronutrients (N, P, Si) are high and most likely are not limiting phytoplankton growth processes at any depth.

(5) Concentrations of dissolved Fe are low (0.05 to ~0.4 nM) in surface waters, as indicated by the data in Table 1.

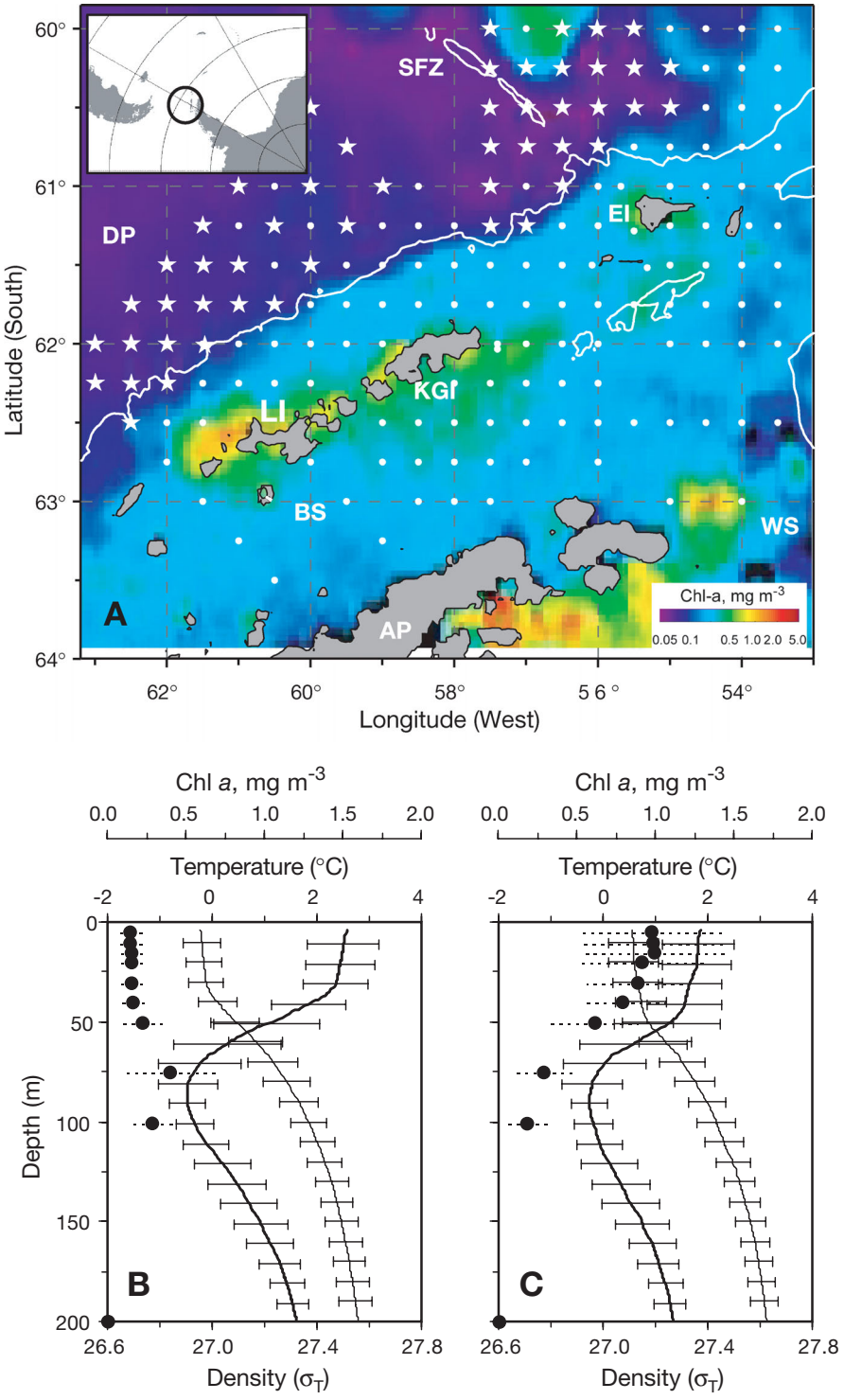

Fig. 1. Location of stations in the AMLR sampling grid and upper water characteristics during the 1997 to 1999 field seasons. (A) Map of the AMLR sampling grid, with all stations having a deep chl *a* maximum indicated by stars and all other stations indicated by small circles. The sampling grid has been superimposed upon a satellite chl *a* image (from Aqua MODIS) of the distribution of chl *a* (mg m^{-3}) in surface waters during January of 2004. The white continuous line is the 2000 m isobath. The inset shows the general location of the AMLR sampling area. (B) Profiles in the upper 200 m of the water column of the 79 stations with a deep chl *a* maximum, showing: the mean chl *a* concentration (●), the mean temperature (thick continuous line), and the mean water density (thin continuous line). (C) Profiles in the upper 200 m of the water column for 21 contiguous stations without a deep chl *a* maximum, showing the mean chl *a* concentration, the mean temperature, and the mean water density. All the horizontal lines in Panels (B) & (C) represent ±SD values at various depths (DP: Drake Passage; SFZ: Shackleton Fracture Zone; EI: Elephant Island; KGI: King George Island; LI: Livingston Island; BS: Bransfield Strait; WS: Weddell Sea; AP: Antarctic Peninsula). Data from Holm-Hansen & Hewes (2004)

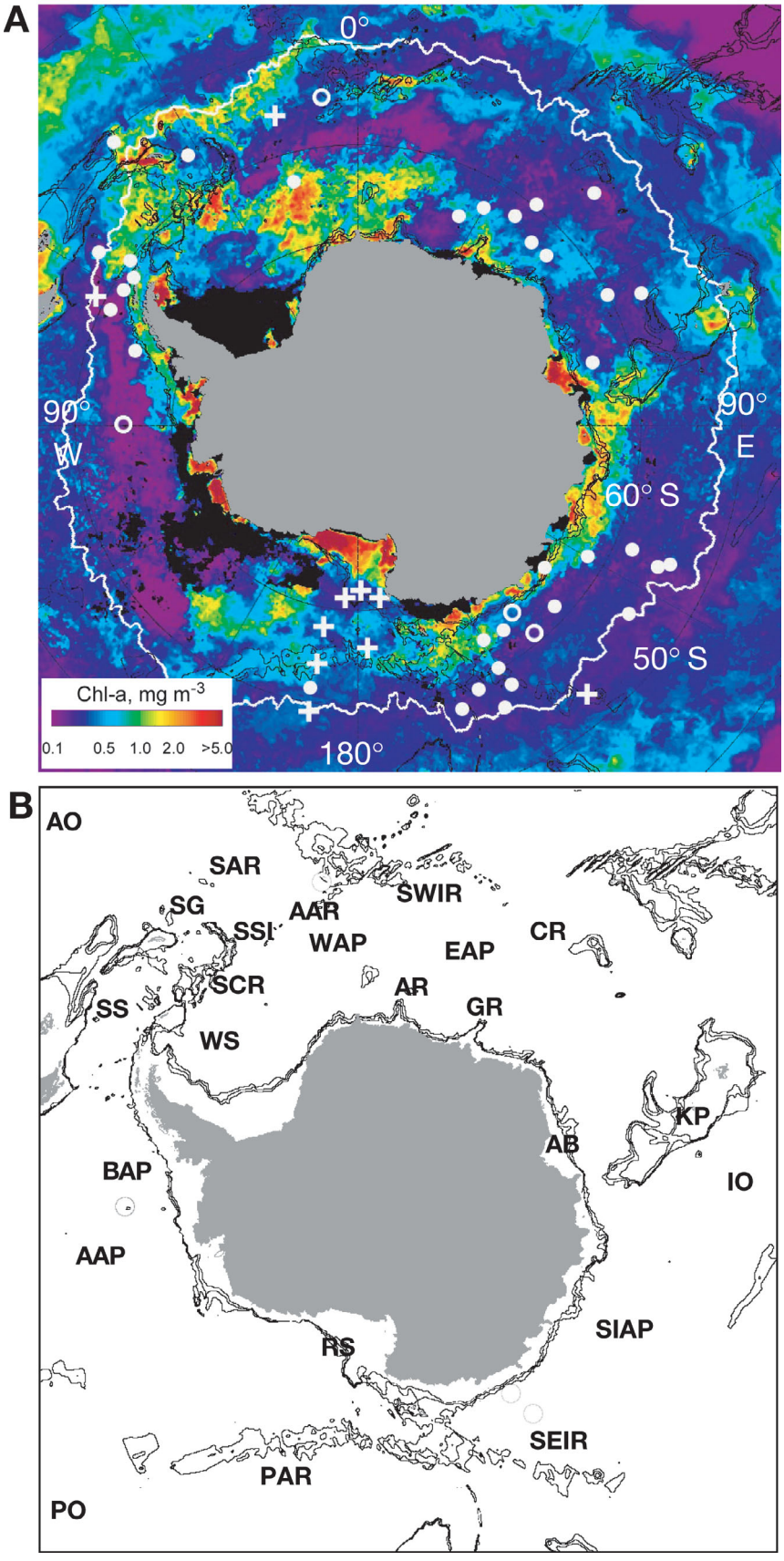

Fig. 2. (A) Satellite image of the Southern Ocean showing distribution of chl *a* (mg m^{-3}) in surface waters during January and February 2000. Data are derived from the Sea-viewing Wide Field-of-view Sensor (SeaWiFS, McClain et al. 1998) using the standard OC4v2 chlorophyll algorithm (O'Reilly et al. 1998, 2000). The jagged white line is the 4°C isotherm, which is the approximate location of the Polar Front. Areas shown in black have insufficient data due to ice cover or to open waters with extensive cloud cover. Major bathymetric features (obtained from the ETOPO2 data base) are shown by the isobaths (thin black lines) for 2000, 2500, and 3000 m depths. The following shipboard acquired data have been added to the chl *a* image: locations where deep chl *a* maxima have been reported (white circles); locations in low chl *a* regions, where dissolved Fe concentrations have been reported (white crosses); and locations where both deep chl *a* maxima and dissolved Fe concentrations have been reported (white rings). Many of the symbols represent multiple stations; in these cases, the symbols shown occupy locations central to the reported stations. The coordinates and references for the chl *a* and Fe data are listed in Table 1. (B) Identification of land and bathymetric features shown in the upper panel; Scotia Sea (SS), the South Scotia Ridge (SCR), Weddell Sea (WS), South Georgia (SG), Atlantic Ocean (AO), South Sandwich Islands (SSI), South Atlantic Ridge (SAR), America Antarctic Ridge (AAR), Weddell Abyssal Plain (WAP), Astrid Ridge (AR), Southwest Indian Ridge (SWIR), Enderby Abyssal Plain (EAP), Gunnerus Ridge (GR), Conrad Rise (CR), Amery Basin (AB), Kerguelen Plateau (KP), Indian Ocean (IO), South Indian Abyssal Plain (SIAP), Southeast Indian Ridge (SEIR), Pacific Antarctic Rise (PAR), Ross Sea (RS), Pacific Ocean (PO), Amundsen Abyssal Plain (AAP), and Bellingshausen Abyssal Plain (BAP)

Table 1. Geographical locations in the Southern Ocean, with cited references, which report deep chl *a* maxima (white circles in Fig. 2), dissolved Fe concentrations in low chl *a* waters (white crosses in Fig. 2), and where both a deep chl *a* maximum and Fe concentrations have been reported (white rings in Fig. 2). All listings in the table are arranged sequentially according to longitude, starting at the prime meridian and progressing first easterly to 180° and then westerly from the prime meridian to the 180° meridian. Where a reference citation reports data from several stations, the coordinates given in the table represent the approximate mid-point of those locations. –: no data

Longitude	Latitude (°S)	Chl *a* (mg m^{-3})	Fe (nM)	Source
25° E	65	0.06	–	Weber & El-Sayed (1987)
30° E	63	0.10	–	Uno (1982)
37° E	62	0.06	–	Watanabe & Nakajima (1982)
39° E	60	0.15	–	Sasaki (1984)
43° E	63	0.30	–	Hattori et al. (1999)
45° E	55	0.20	–	Watanabe & Nakajima (1982)
48° E	63	0.20	–	Uno (1982)
62° E	60	0.10	–	Fiala et al. (1998)
66° E	57	0.20	–	Treguer & Jacques (1992)
75° E	64	0.10	–	Fukui et al. (1986)
114° E	54	0.30	–	Holm-Hansen et al. (1977)
115° E	55	0.20	–	El-Sayed & Fryxell. (1993)
115° E	58	0.30	–	El-Sayed & Jitts (1973)
120° E	62	0.20	–	Yamaguchi et al. (1985)
125° E	55	0.20	–	Yamaguchi & Shibata (1982)
135° E	62	0.20	–	Hirawake et al. (2000)
140° E	53	–	0.30	Sedwick et al. (1997)
140° E	61	0.30	–	Trull et al. (2001)
140° E	61	0.25	0.08	Boyd et al. (2000)
140° E	64	0.20	0.20	Sohrin et al. (2000)
145° E	63	0.10	–	Yamaguchi et al. (1985)
150° E	58	0.07	–	Holm-Hansen et al. (1977)
150° E	61	0.15	–	Odate & Fukuchi (1995)
150° E	63	0.10	–	Yamaguchi et al. (1985)
153° E	56	0.10	–	El-Sayed (1970)
156° E	59	0.10	–	El-Sayed (1970)
160° E	58	0.20	–	Yamaguchi & Shibata (1982)
173° E	72	–	0.05	Fitzwater et al. (2000)
177° E	73	–	0.05	Fitzwater et al. (2000)
178° E	66	–	0.15	Sedwick et al. (2000)
6° W	55	0.25	0.49	De Baar et al. (1995)
15° W	56	–	0.60	Löscher et al. (1997)
15° W	63	0.05	–	Mikaelya & Belyaeva (1995)
32° W	56	0.20	–	Holm-Hansen et al. (2004)
40° W	52	0.68	–	Gilpin et al. (2002)
54° W	60	0.50	–	Figueiras et al. (1998)
56° W	57	0.10	–	El-Sayed & Weber (1982)
57° W	63	0.15	–	Mikaelya & Belyaeva (1995)
60° W	61	0.10	–	Holm-Hansen & Hewes (2004)
64° W	59	–	0.16	Martin et al. (1990a)
65° W	61	0.08	–	Lipski (1982)
71° W	65	0.20	–	Garibotti et al. (2003)
91° W	65	0.05	0.17	de Baar et al. (1999)
170° W	59	0.29	0.06	Franck et al. (2003)
170° W	62	0.20	–	DiTullio et al. (2003)
170° W	64	–	0.10	Measures & Vick (2001)
170° W	68	0.96	0.02	Franck et al. (2003)
174° W	72	–	0.10	Johnson et al. (1997)

(6) Relatively few papers report profiles of solar irradiance at the stations where DCMs are located, but, from available data (e.g. Holm-Hansen & Hewes 2004), the light levels at the top, middle, and bottom of the DCM are approximately 7.8, 2.3, and 0.3% of the solar irradiance incident upon the sea surface. Comparable percentages at the same depths at contiguous stations that have higher chl *a* concentrations in the UML, but no DCM at depth are 2.6, 0.6, and 0.1% of incident solar radiation.

Relation of DCMs to the TML

Data in Fig. 1B show that the DCM is found within the TML, but that the depth of the maximum chl *a* concentration is generally slightly shallower than the depth of the temperature minimum. These findings are similar to those reported by Uno (1983). The TML occurs in all Antarctic pelagic waters and extends from close to the continental shelf break north as far as the Polar Front. The TML is the winter remnant of the AASW, which is deeply mixed (>100 m) during the winter period. During winter, phytoplankton biomass and rate of assimilation of nutrients will be very low due to low incident solar irradiance and deep mixing of the UML (Sakshaug et al. 1991). At the end of the winter period, nutrient concentrations will be relatively high and uniform within this deeply mixed and isothermal upper water column. The seasonal formation of the DCM as suggested by Holm-Hansen & Hewes (2004) depends upon the following processes: (1) During spring and early summer increasing solar irradiance results in heating of surface waters; during the summer months of January–March there is thus a relatively shallow UML of <50 m, which overlies the colder remnant of the winter water. (2) With high solar irradiance during the summer months, phytoplankton biomass increases in this UML of <50 m and will draw down the dissolved Fe concentrations to very low concentrations (<0.1 nM). (3) Grazing of phytoplankton by zooplankton and krill will result in loss of particulate organic material containing Fe from the upper water

column. (4) If the chl *a* concentrations stabilize at fairly low concentrations (< 0.2 mg m^{-3}) in this UML, the irradiance in the underlying remnant of the winter water will be sufficiently high to support increased phytoplankton biomass due to higher initial levels of Fe. (5) As phytoplankton growth in the TML will be light-limited, the chl *a* maximum will be in the upper portion of the UML, with decreasing phytoplankton biomass in the lower portions of the TML. Finally, (6) development of a DCM as described above is dependent upon the formation of a UML of less than ~50 m overlying the TML. Data of Trull et al. (2001) and Sprintall (2003) indicate that the TML forms during December, which means that a well-defined DCM would be evident only from December and through the summer months. This is consistent with all the references reporting DCMs in Table 1, as most of those papers show DCMs in January and February, with just a few papers reporting DCMs in late December or early March.

It is seen from Fig. 2 that large pelagic areas of Antarctic waters have elevated chl *a* concentrations and no reported DCMs, in spite of the presence of a TML. The reason for this is most likely the fact that, when chl *a* concentrations are greater than ~0.8 mg m^{-3}, the increased rate of attenuation of solar radiation in the UML results in irradiances in the TML that are not high enough to permit significant phytoplankton growth (Holm-Hansen & Hewes 2004). From data on Fe concentrations in Antarctic waters (see De Baar & de Jong 2001), the relatively high phytoplankton biomass in the UML in these regions can be correlated with increased Fe concentrations in the UML. Processes responsible for such increased Fe concentrations are discussed in a later section.

Dissolved Fe concentrations in Antarctic waters

There have been relatively few studies of dissolved Fe concentrations in the low chl *a* regions of the Southern Ocean. As can be seen from Fig. 2 and Table 1, data on dissolved Fe are primarily from 3 regions: (1) the area from 6 to 90° W, studied mostly by German and Dutch researchers; (2) the area centered at 140° E, studied by Australian and New Zealand personnel; and (3) the Ross Sea region, studied by the US JGOFS program. Dissolved Fe concentrations in surface waters in these regions are mostly in the range of 0.1 to 0.3 nM. The regions with elevated chl *a* concentrations (see Fig. 2) generally have much higher concentrations of dissolved Fe. Examples include Fe concentrations of 7.4 nM in Gerlache Strait (Martin et al. 1990a), 4.0 to 31 nM in the Bransfield Strait area (Sañudo-Wilhelmy et al. 2002), 1.1 to 2.1 nM in the Weddell Sea (Westerlund & Öhman 1991, Sañudo-Wilhelmy et al. 2002), 2 to 8 nM in the Scotia Sea and 60 nM over the South Orkney shelf (Nolting et al. 1991), >1.0 nM in the Ross Sea (Martin et al. 1991, Fitzwater et al. 2000), and 1.1 to 1.9 nM in the Polar Front region at 6° W (Löscher et al. 1997). Dissolved Fe concentrations increase with depth in the Southern Ocean (Löscher et al. 1997, Measures & Vick 2001) and show a typical nutrient-like profile as described by Johnson et al. (1997).

The Fe concentrations listed above refer only to the 'dissolved Fe', which is generally measured on filtrates passed through a polycarbonate filter with pore diameters of 0.4 µm and is commonly the only component of the total Fe present in the water sample that is measured. This 'dissolved Fe' is believed to be the most relevant component of the total Fe present in any water sample for assimilation by phytoplankton (Löscher et al. 1997); hence, Table 1 does not include data on 'total dissolvable Fe', 'labile Fe', or 'total particulate Fe'. Furthermore, as so little is known about the degree and strength of complexation of Fe with inorganic and organic ligands in Antarctic waters, we have restricted the Fe data in the table to the dissolved Fe component. Data of Fe chemistry in marine waters have recently been summarized and discussed by De Baar & de Jong (2001).

Relationship between chl *a* and Fe concentrations in regard to bathymetry and mixing processes

It is seen from the locations of the stations having a DCM that they are found in or close to 4 major deep-basin regions of the Southern Ocean that have very low chl *a* concentrations (Figs. 2 & 3). These 4 regions are: (1) the abyssal plains of the Amundsen and Bellingshausen Seas (~70 to 140° W), (2) the Weddell Abyssal Plain (~20° W to 20° E), (3) the Enderby Abyssal Plain (~20 to 60° E), and (4) the South Indian Abyssal Plain (~110 to 150° E).

The mean Fe concentration in these low chl *a* waters at the stations shown in Fig. 2 is ~0.17 nM. The major sources of Fe in surface waters are generally from (1) coastal and shelf waters, which are enriched from bottom sediments and run-off from land (De Baar et al. 1990, 1995, Nolting et al. 1991); (2) upwelling of deeper waters, which generally have considerably higher Fe concentrations (De Baar et al. 1995, Measures & Vick 2001, Watson 2001); (3) melting of annual sea ice (Fitzwater et al. 2000, Arrigo et al. 2003); (4) mixing associated with frontal systems (Moore & Abbott 2000); and (5) aeolian input from the atmosphere (Duce & Tindale 1991, Martin et al. 1991). Aeolian input of Fe in Antarctic waters, however, seems to be minimal (Watson 2001), with most of the Fe in surface waters coming from either coastal waters or by upwelling processes

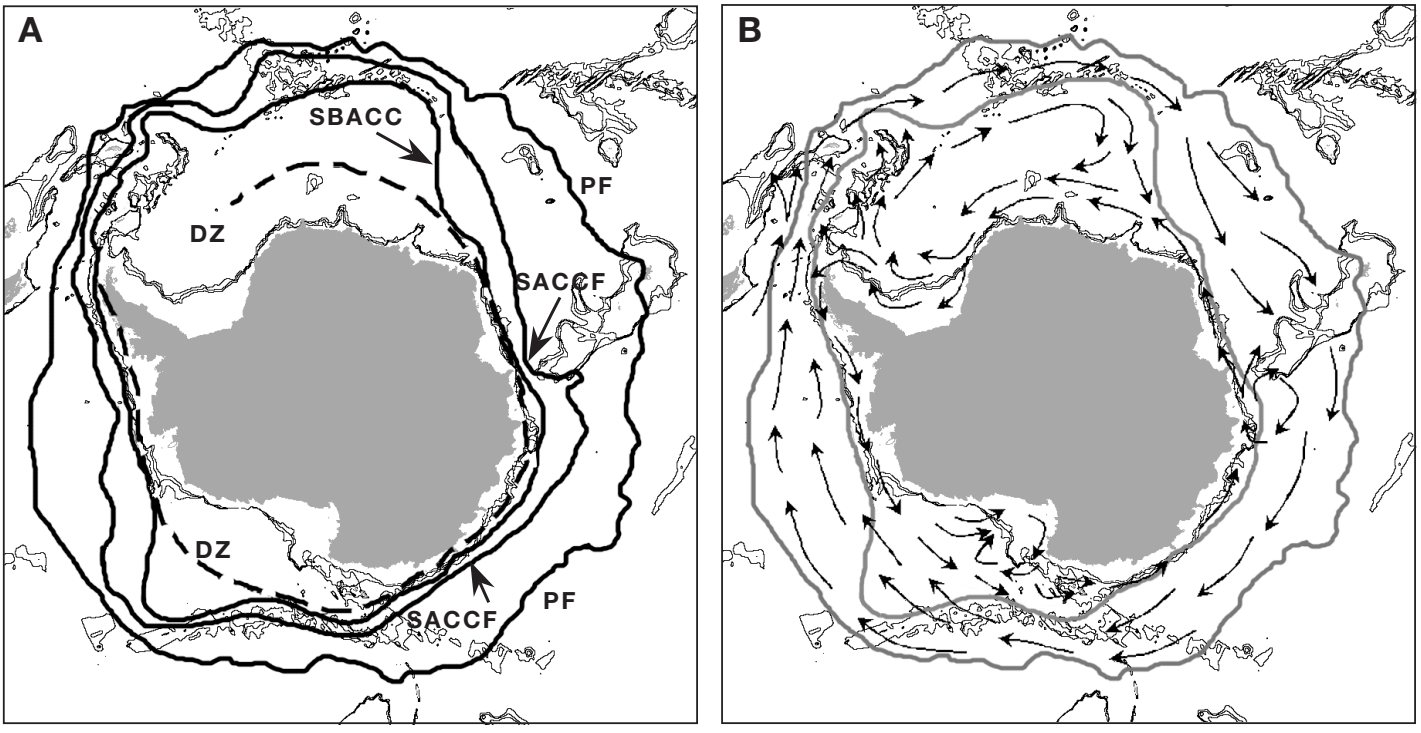

Fig. 3. (A) Map of the identical geographical region illustrated in Fig. 2, but showing the locations of various oceanographic frontal zones, in addition to the major bathymetric features. The zones indicated are the Southern Boundary Antarctic Circumpolar Current (SBACC), the Southern Antarctic Circumpolar Current Front (SACCF), the Polar Front (PF), and the Divergence Zone (DZ). Locations of the frontal systems were based on papers by Deacon (1982), Orsi et al. (1993, 1995), Knox (1994), Hofmann et al. (1998), and Park et al. (1998). (B) Map of the identical geographical region illustrated in Fig. 2, with arrows indicating a generalized view of the direction of surface-water flow in relation to the major frontal systems. It should be noted that data obtained from drifters generally show very complex circulation patterns, with many eddies and changes in water-flow direction; hence, the water flow as indicted by the arrows must be viewed as being very schematic. Data on circulation were based on papers by Knox (1994), Hofmann et al. (1998), and Nicol et al. (2000)

that are often related to bathymetric features (Moore et al. 1999a, Watson 2001).

Waters over coastal shelf areas generally have high chl *a* concentrations (Fig. 2) and also have considerably higher Fe concentrations in surface waters as referenced above. The shelf regions with very high chl *a* concentrations include: (1) portions of the Weddell Sea that are not covered with ice; (2) the shelf and northerly projecting Astrid Ridge, close to 10° E, 67° S; (3) Gunnerus Bank and Gunnerus Ridge, close to 30° E; (4) the shelf and banks of Amery Basin, between 70 and 80° E; (5) the coastal region from ~90 to 115° E, 63 to 65° S, which has many relatively shallow banks and islands (Nicol et al. 2000); (6) shelf portions of the Ross Sea; (7) the Amundsen Sea, between 100 and 120° W; (8) the Bellingshausen Sea, between 75 and 90° W; (9) portions of the Scotia Ridge and Endurance Ridge, between 30 to 37° W and 60 to 63° S; and (10) the shelves of South Georgia and Shag Rocks, between 37 to 42° W and 53 to 56° S.

Reports by various investigators have shown that chl *a* concentrations are often relatively high over sea mounts and ridges, which rise to within ~2000 m of the sea surface (Sullivan et al. 1993, Moore et al. 1999a, Constable & Nicol 2003). Garabato et al. (2004) have also provided physical data showing that turbulent mixing over rough topography in the Southern Ocean could be an important process in the upward transport of Fe-enriched deep water. It is thus likely that the elevated phytoplankton biomass found in many regions of pelagic Antarctic waters is due to the enrichment of surface waters with Fe resulting from upwelling processes associated with the deep currents of the ACC impacting bathymetric features. Fig. 3 shows the major bathymetric features in Antarctic waters, in relation to the location of important oceanic fronts and major currents. In comparing Figs. 2 & 3, it is seen that the major pelagic areas with high chl *a* concentrations either are in close proximity to shelf waters or have complex topographical features, both of which may be responsible for enrichment of surface waters with Fe. The high chl *a* pelagic regions seen in Fig. 2 include:

(1) The Scotia Sea, which is delimited by South Georgia in the north, the South Orkney Islands in the south, the South Sandwich Islands in the east, and by the 55° W meridian. The waters of the Scotia Sea have

sufficiently high concentrations of Fe (~2 nM; Nolting et al. 1991) so that phytoplankton biomass is not limited by Fe availability (De Baar et al. 1990). It is likely that the high Fe concentrations in the Scotia Sea result partly from the inflow of Fe-enriched waters from shelf regions (e.g. coastal regions to the north of the South Shetland Islands, Bransfield Strait, the entire Scotia Ridge, and the Weddell Sea), as mentioned by De Baar et al. (1995), as well as from inflow of Weddell Sea Deep Water through 4 deep passages, as described by Heywood et al. (2002). Garabato et al. (2004) have also described eddies and upwelling of Fe-enriched deep water in the Scotia Sea that are related to the complex bottom topography of this region.

(2) The Polar Front Zone (PFZ) between South Georgia (~37° W) and the 10° W meridian, as shown in Fig. 2. De Baar et al. (1995) have shown that Fe concentrations in this PFZ at ~6° W are high (~2 nM), as compared to lower values (~0.5 nM) in the low chl *a* region to the south at ~57° S. These authors, as well as Löscher et al. (1997), Atkinson et al. (2001), and Whitehouse et al. (2000) have attributed the high Fe content of the waters in this PFZ both to shelf sediments around South Georgia and the Scotia Ridge, as well as to upwelling processes associated with the PFZ jet (De Baar et al. 1995).

(3) The area from 20° E to 30° W and 60 to 70° S, which is south of the Scotia Front (Belkin & Gordon 1996) and within the Weddell Sea gyre and the East Wind Drift (see Fig. 3). This area also includes the Isles Orcadas Seamounts and Maud Rise (~3° E, 65° S). Fe concentrations are relatively high in the Weddell Sea (Westerlund & Öhman 1991), and, consequently, the ice-free waters of the Weddell Sea gyre can be expected to have relatively high phytoplankton biomass.

(4) The high chl *a* area located from approximately 8° W to 20° E and 52 to 56° S, which overlies the eastern end of the America Antarctic Ridge, the southern portion of the Mid-Atlantic Ridge, and much of the Southwest Indian Ridge.

(5) The high chl *a* area from ~65 to 75° E, 50 to 56° S, which overlies shelf and deep waters around Iles Kerguelen.

(6) The area from ~80 to 90° E, 55 to 64° S, which overlies the southern portion of the Kerguelen Plateau, which rises to depths of <1000 m. Waters downstream of the Kerguelen Plateau are also high in chl *a*, as suggested by Blain et al. (2001).

(7) The area from ~145 to 170° E, 62 to 66° S, which overlies a relatively shallow area of the Southern Ocean (mostly <3000 m) and includes complex bottom topography, with many islands, banks, and seamounts.

(8) The area from 135 to 170° W, 62 to 72° S, which is immediately downstream of: (a) the broad Pacific Antarctic Ridge, with its many fracture zones and seamounts rising to <2500 m, and (b) many islands and seamounts in the region from 160 to 180° E.

DISCUSSION

The data presented above, coupled with data in Holm-Hansen & Hewes (2004), indicate that DCMs are found only in regions where chl *a* concentrations are very low in the UML, and that they are not found in regions where chl *a* concentrations in the UML are higher than ~0.8 mg m^{-3}. The hypothesis that the formation of a DCM is indicative of low Fe concentrations in surface waters is supported by direct measurements of Fe concentrations (e.g. Martin et al. 1990b, De Baar & de Jong 2001) and also by Fe-addition experiments, either in on-deck incubations (e.g. Martin et al. 1990b, Helbling et al. 1991, Scharek et al. 1997, Van Leeuwe et al. 1997, Timmermans et al. 1998) or by release of large amounts of Fe to surface waters (e.g. Boyd & Law 2001). Addition of Fe to water samples from areas with chl *a* concentrations greater than ~0.8 mg m^{-3} (which includes both coastal areas and pelagic regions) have not shown any increase in phytoplankton biomass as a result of Fe addition (De Baar et al. 1990, Martin et al. 1990b, Helbling et al. 1991). It should be noted that some of the above studies demonstrating Fe limitation of phytoplankton growth in the AMLR study area (e.g. Helbling et al. 1991) are immediately adjacent to the location where Martin et al. (1990a,b) reported very low concentrations of dissolved Fe (0.16 nM). It thus seems a reasonable hypothesis that (1) the low chl *a* concentrations in the 3 major large deep-basin regions of the Southern Ocean (Southern Pacific Ocean, Southwest Indian Ocean, and Southeast Indian–Australian sector) result from growth-limiting Fe concentrations in the euphotic zone, as these deep basins get relatively little enrichment of Fe from sediments or upwelling processes, (2) the DCMs found embedded in the TML in these 3 low chl *a* regions reflect limiting Fe concentrations in the UML and higher Fe concentrations in the winter remnant of the AASW, and (3) no DCMs related to Fe limitation occur in shelf or coastal waters.

The distribution of chl *a* in Antarctic waters seen in Fig. 2 seems to be inter-annually consistent, based both on shipboard data and on satellite chl *a* images from other years (e.g. Comiso et al. 1993, Sullivan et al. 1993, Moore at al. 1999a, Moore & Abbott 2000). This is not surprising, as the high chl *a* regions apparently are not Fe-limited, due to enrichment of Fe either from Fe-rich coastal and shelf waters or from deep water by upwelling processes associated with bathymetric features. This consistency of high-production regions can

be expected to be important in the distribution and biomass of higher trophic levels, which are important in regard to harvestable resources in the Southern Ocean. Support for this is shown by the distribution of krill *Euphausia superba*, which have been shown to be in high density in (1) the Scotia Sea, (2) the eastern portion of the Weddell Sea gyre, (3) the Eastwind Drift from about 10 to 50° E, (4) the small gyre and Eastwind Drift from about 90 to 120° E, (5) the area of the Ross Sea gyre, and (6) shelf regions of the Bellingshausen Sea (Marr 1962, Priddle et al. 1988, Everson & Miller 1994). It should be noted that many investigators have previously related krill density either to location in the Eastwind Drift (e.g. Amos 1984) or to gyre systems (e.g. Marr 1962). Conclusions regarding available food resources for zooplankton based on recent phytoplankton-chemical studies agree well with the historical distribution of krill based on direct netting and bioacoustic estimates. Thus, information acquired during the past decade from new technologies such as remote sensing, as well as through improvements in determining concentrations of essential micro-elements such as Fe, has provided insight into the underlying factors of importance for productivity at all trophic levels in the Southern Ocean.

Acknowledgements. This work was partly funded through the US AMLR program, administered by the Antarctic Ecosystem Research Division at NOAA's Southwest Fisheries Research Center, La Jolla, California. M.K. was supported by NSF Grant 0230443 to B. G. Mitchell and by the NASA Ocean Biogeochemistry Program. The report was prepared by O.H.-H. and C.D.H. under Award No. NA17RJ1231 from the National Oceanic and Atmospheric Administration, US Department of Commerce. The statements, findings, conclusions, and recommendations are those of the authors and do not necessarily reflect the views of the National Oceanic and Atmospheric Administration or the Department of Commerce.

LITERATURE CITED

Amos AF (1984) Distribution of krill (*Euphausia superba*) and the hydrography of the Southern Ocean: large-scale processes. J Crustac Biol 4(Spec No. 1):306–329

Arrigo KR, Worthen DL, Robinson DH (2003) A coupled ocean–ecosystem model of the Ross Sea. 2. Iron regulation of phytoplankton taxonomic variability and primary production. J Geophys Res 108(C7):3231(24,1–17)

Atkinson A, Whitehouse MJ, Priddle J, Cripps GC, Ward P, Brandon MA (2001) South Georgia, Antarctica: a productive, cold water, pelagic ecosystem. Mar Ecol Prog Ser 216: 279–308

Belkin IM, Gordon AL (1996) Southern Ocean fronts from the Greenwich meridian to Tasmania. J Geophys Res 101 (C2):3675–3696

Berdalet E, Vaque D, Arin L, Estrada M, Alcaraz M, Fernandez JA (1997) Hydrography and biochemical indicators of microplankton biomass in the Bransfield Strait (Antarctica) during January 1994. Polar Biol 17:31–38

Blain S, Tréguer P, Belviso S, Bucciarelli E and 9 others (2001) A biogeochemical study of the island mass effect in the context of the iron hypothesis: Kerguelen Islands, Southern Ocean. Deep-Sea Res I 48:163–187

Boyd PW, Law CS (2001) The Southern Ocean Iron RElease Experiment (SOIREE)—introduction and summary. Deep-Sea Res II 48:2425–2438

Boyd PW, Watson AJ, Law CS, Abraham ER and 31 others (2000) A mesoscale phytoplankton bloom in the polar Southern Ocean stimulated by iron fertilization. Nature 407:695–702

Chamberlin WS, Booth CR, Kiefer DA, Morrow JH, Murphy RC (1990) Evidence for a simple relationship between natural fluorescence, photosynthesis and chlorophyll in the sea. Deep-Sea Res 37:951–973

Chisholm SW, Morel FMM (eds) (1991) What controls phytoplankton production in nutrient-rich areas of the open sea? Limnol Oceangr 36(8):1507–1970

Comiso JC, McClain CR, Sullivan CW, Ryan JP, Leonard CL (1993) Coastal Zone Color Scanner pigment concentrations in the Southern Ocean and relationships to geophysical surface features. J Geophys Res 98:2419–2451

Constable AJ, Nicol S (2003) Southern Ocean productivity in relation to spatial and temporal variation in the physical environment. J Geophys Res 108(C4):8079

Deacon GER (1982) Physical and biological zonation in the Southern Ocean. Deep-Sea Res 29(1A):1–15

De Baar HJW, de Jong JTM (2001) Distributions, sources and sinks of iron in seawater. In: Turner DR, Hunter KA (eds) The biogeochemistry of iron in seawater. John Wiley & Sons, London, p 123–253

De Baar HJW, Buma AGJ, Nolting RF, Cadee GC, Jacques G, Treguer PJ (1990) On iron limitation of the Southern Ocean: experimental observations in the Weddell and Scotia Seas. Mar Ecol Prog Ser 65:105–122

De Baar HJW, de Jong JTM, Bakker DCE, Löscher BM, Veth C, Bathmann U, Smetacek V (1995) Importance of iron for plankton blooms and carbon dioxide drawdown in the Southern Ocean. Nature 373:412–415

De Baar HJW, de Jong JTM, Nolting RF, Timmermans KR, van Leeuwe MA, Bathmann U, van der Loeff MR, Sildam J (1999) Low dissolved Fe and the absence of diatom blooms in remote waters of the Southern Ocean. Mar Chem 66:1–34

DiTullio GR, Geesey ME, Jones DR, Daly KL, Campbell L, Smith WO Jr (2003) Phytoplankton assemblage structure and primary productivity along 170° W in the South Pacific Ocean. Mar Ecol Prog Ser 255:55–80

Duce RA, Tindale NW (1991) Atmospheric transport of iron and its deposition in the ocean. Limnol Oceanogr 36: 1715–1726

El-Sayed SZ (1970) On the productivity of the Southern Ocean. In: Holdgate MW (ed) Antarctic ecology. Academic Press, London, p 119–135

El-Sayed SZ, Fryxell GA (1993) Phytoplankton. In: Friedman I (ed) Antarctic microbiology. Wiley-Liss, New York, p 65–122

El-Sayed SZ, Jitts HR (1973) Phytoplankton production in the southwestern Indian Ocean. In: Zeitzschel B (ed) Ecological studies. Analysis and synthesis. Springer-Verlag, Berlin, p 131–142

El-Sayed SZ, Weber LH (1982) Spatial and temporal variations in phytoplankton biomass and primary productivity in the Southwest Atlantic and the Scotia Sea. Polar Biol 1: 83–90

Everson I, Miller DGM (1994) Krill distribution and abundance: results and implications of research during the BIOMASS Programme. In: El-Sayed SZ (ed) Southern

Ocean ecology. Cambridge University Press, Cambridge, p 129–143
Fiala M, Semeneh M, Oriol L (1998) Sized-fractionated phytoplankton biomass and species composition in the Indian sector of the Southern Ocean during austral summer. J Mar Syst 17:179–194
Figueiras FG, Estrada M, Lopez O, Arbones B (1998) Photosynthetic parameters and primary production in the Bransfield Strait: relationships with mesoscale hydrographic structures. J Mar Syst 17:129–141
Fitzwater SE, Johnson KS, Gordon RM, Coale KH, Smith WO Jr (2000) Trace metal concentrations in the Ross Sea and their relationship with nutrients and phytoplankton growth. Deep-Sea Res II 47:3159–3179
Franck VM, Bruland KW, Hutchins DA, Brzezinski MA (2003) Iron and zinc effects on silicic acid and nitrate uptake kinetics in three high-nutrient, low-chlorophyll (HNLC) regions. Mar Ecol Prog Ser 252:15–33
Fukui F, Otomo K, Okabe S (1986) Nutrients depression in the blooming area of Prydz Bay, Antarctica. Mem Natl Inst Polar Res (Spec Issue) 44:43–54
Garabato ACN, Polzin KL, King BA, Heywood KJ, Visbeck M (2004) Widespread intense turbulent mixing in the Southern Ocean. Science 303:210–213
Garibotti IA, Vernet M, Ferrario ME, Smith RC, Ross RM, Quetin LB (2003) Phytoplankton spatial distribution patterns along the western Antarctic peninsula (Southern Ocean). Mar Ecol Prog Ser 261:21–39
Gilpin LC, Priddle J, Whitehouse MJ, Savidge G, Atkinson A (2002) Primary production and carbon uptake dynamics in the vicinity of South Georgia — balancing carbon fixation and removal. Mar Ecol Prog Ser 242:51–62
Hattori H, Tanimura A, Fukuchi M (1999) Vertical distribution of size fractionated phytoplankton chlorophyll in the Indian sector of the Southern Ocean in summer (1985/86). Polar Biosci 12:15–25
Helbling EW, Villafañe V, Holm-Hansen O (1991) Effect of Fe on productivity and size distribution of Antarctic phytoplankton. Limnol Oceanogr 36:1879–1885
Heywood KJ, Naveira Garabato AC, Stevens DP (2002) High mixing rates in the abyssal Southern Ocean. Nature 415: 1011–1014
Hirawake T, Satoh H, Ishimaru T, Yamaguchi Y (2000) Photosynthetic characteristics of phytoplankton off Adelie Land, Antarctica, during the austral summer. Polar Biosci 13: 28–42
Hofmann EE, Klinck JM, Locarnini RA, Fach B, Murphy E (1998) Krill transport in the Scotia Sea and environs. Antarc Sci 10(4):406–415
Holm-Hansen O, Hewes CD (2004) Deep chlorophyll-*a* maxima (DCMs) in Antarctic waters. I. Relationships between DCMs and the physical, chemical, and optical conditions in the upper water column. Polar Biol 27:699–710
Holm-Hansen O, El-Sayed SZ, Franceschini GA, Cuhel RL (1977) Primary production and the factors controlling phytoplankton growth in the Southern Ocean. In: Llano GA (ed) Adaptations within Antarctic ecosystems: proceedings of the 3rd SCAR symposium on Antarctic biology. Gulf Publishing, Houston, TX, p 11–50
Holm-Hansen O, Mitchell BG, Hewes CD, Karl DM (1989) Phytoplankton blooms in the vicinity of Palmer Station, Antarctica. Polar Biol 10:49–57
Holm-Hansen O, Helbling EW, Lubin D (1993) Ultraviolet radiation in Antarctica: inhibition of primary production. Photochem Photobiol 58P:567–570
Holm-Hansen O, Naganobu M, Kawaguchi S, Kameda T and 9 others (2004) Factors influencing the distribution, biomass, and productivity of phytoplankton in the Scotia Sea and adjoining waters. Deep-Sea Res II 51:1333–1350
Johnson KS, Gordon RM, Coale KH (1997) What controls dissolved iron concentrations in the world ocean? Mar Chem 57:137–161
Kiefer DA, Chamberlin WS, Booth CR (1989) Natural fluorescence of chlorophyll *a*: relationship to photosynthesis and chlorophyll concentration in the western South Pacific gyre. Limnol Oceanogr 34:868–881
Knox GA (1994) The biology of the Southern Ocean. Cambridge University Press, Cambridge
Lipski M (1982) The distribution of chlorophyll-*a* in relation to the water masses in the southern Drake Passage and the Bransfield Strait (BIOMASS-FIBEX, February–March 1981). Pol Polar Res 3(3–4):143–152
Löscher BM, de Baar HJW, de Jong JTM, Veth C, Dehairs F (1997) The distribution of Fe in the Antarctic Circumpolar Current. Deep-Sea Res II 44(1–2):143–187
Marr JWS (1962) The natural history and geography of the Antarctic krill (*Euphausia superba* Dana). Discovery Rep 32:33–464
Martin JH, Gordon RM, Fitzwater SE (1990a) Iron in Antarctic waters. Nature 345:156–158
Martin JH, Fitzwater SE, Gordon RM (1990b) Iron deficiency limits phytoplankton growth in Antarctic waters. Global Biogeochem Cycles 4:5–12
Martin JH, Gordon RM, Fitzwater SE (1991) The case for iron. Limnol Oceanogr 36(8):1793–1802
McClain CR, Cleave ML, Feldman GC, Gregg WW, Hooker SB, Kuring N (1998) Science quality SeaWiFS data for global biosphere research. Sea Technol 39(9):10–16
Measures CI, Vick S (2001) Dissolved Fe in the upper waters of the Pacific sector of the Southern Ocean. Deep-Sea Res II 48:3913–3941
Mikaelyan AS, Belyaeva GA (1995) Chlorophyll '*a*' content in cells of Antarctic phytoplankton. Polar Biol 15:437–445
Moore JK, Abbott MR (2000) Phytoplankton chlorophyll distributions and primary production in the Southern Ocean. J Geophys Res 105(C-12):28709–28722
Moore JK, Abbott MR, Richman JG, Smith WO, Cowles TJ, Coale KH, Gardner WD, Barber RT (1999a) SeaWiFS satellite ocean color data from the Southern Ocean. Geophys Res Lett 26(10):1465–1468
Moore JK, Abbott MR, Richman JG (1999b) Location and dynamics of the Antarctic Polar Front from satellite sea surface temperature data. J Geophys Res 104:3059–3073
Nelson DM, Smith WO Jr (1986) Phytoplankton bloom dynamics of the western Ross Sea ice edge. II. Mesoscale cycling of nitrogen and silicon. Deep-Sea Res 33: 1389–1412
Nicol S, Pauly T, Bindoff NL, Strutton PG (2000) 'BROKE:' a biological/oceanographic survey off the coast of East Antarctica (80–150° E) carried out in January–March 1996. Deep-Sea Res II 47:2281–2298
Nolting RF, de Baar HJW, Van Bennekom AJ, Masson A (1991) Cadmium, copper, and iron in the Scotia Sea, Weddell Sea and Weddell/Scotia Confluence (Antarctica). Mar Chem 35:219–243
Odate T, Fukuchi M (1995) Distribution and community structure of the picophytoplankton in the Southern Ocean during the late austral summer of 1992. Polar Biol 8:86–100
O'Reilly JE, Maritorena S, Mitchell BG, Siegel DA, Carder KL, Garver SA, Kahru M, McClain C (1998) Ocean color chlorophyll algorithms for SeaWiFS. J Geophys Res 103: 24,937–24,953
O'Reilly JE, Maritorena S, Siegel DA, O'Brien MC and 18 others (2000) Ocean color chlorophyll *a* algorithms for SeaWiFS,

OC2, and OC4: version 4. In: Hooker SB, Firestone ER (eds) SeaWiFS postlaunch calibration and validation analyses. Part 3. National Aeronautics and Space Administration Technical Memorandum 2000–206892, Vol 11. NASA Goddard Space Flight Center, Greenbelt, MD, p 9–23

Orsi AH, Nowlin WD Jr, Whitworth T III (1993) On the circulation and stratification of the Weddell Gyre. Deep-Sea Res I 40:169–203

Orsi AH, Whitworth T III, Nowlin WD Jr (1995) On the meridional extent and fronts of the Antarctic Circumpolar Current. Deep-Sea Res 42(5):641–673

Park YH, Charriaud E, Fieux M (1998) Thermohaline structure of the Antarctic Surface Water/Winter Water in the Indian sector of the Southern Ocean. J Mar Syst 17:5–23

Priddle J, Croxall JP, Everson I, Heywood RB, Murphy EJ, Prince PA, Sear CB (1988) Large-scale fluctuation in distribution and abundance of krill — a discussion of possible causes. In: Sahrhage D (ed) Antarctic Ocean and resources variability. Springer-Verlag, Berlin, p 169–182

Sakshaug E, Slagstad D, Holm-Hansen O (1991) Factors controlling the development of phytoplankton blooms in the Antarctic Ocean—a mathematical model. Mar Chem 35: 259–271

Sañudo-Wilhelmy SA, Olsen KA, Scelfo JM, Foster TD, Flegal AR (2002) Trace metal distributions off the Antarctic Peninsula in the Weddell Sea. Mar Chem 77:157–170

Sasaki H (1984) Distribution of nano- and microplankton in the Indian sector of the Southern Ocean. Mem Natl Inst Polar Res (Spec Issue) 32:38–50

Scharek R, Van Leeuwe MA, De Baar HJW (1997) Responses of Antarctic phytoplankton to the addition of trace metals. Deep-Sea Res II 44:209–228

Sedwick PN, Edwards PR, Mackey DJ, Griffiths FB, Parslow JS (1997) Iron and manganese in surface waters of the Australian subantarctic region. Deep-Sea Res II 44:1239–1253

Sedwick PN, DiTullio GRT, Mackey DJ (2000) Iron and manganese in the Ross Sea, Antarctica: seasonal iron limitation in Antarctic shelf waters. J Geophys Res 105(C5): 11,321–11,336

Smith RC, Cullen JJ (1995) Effects of UV radiation on phytoplankton. Rev Geophys Suppl(July):1211–1223

Sohrin Y, Iwamoto S, Matsui M, Obata H, Nakayama E, Suzuki K, Handa N, Ishii M (2000) The distribution of Fe in the Australian sector of the Southern Ocean. Deep-Sea Res I 47:55–84

Sprintall J (2003) Seasonal to interannual upper-ocean variability in the Drake Passage. J Mar Res 61:27–57

Sullivan CW, Arrigo KR, McClain CR, Comiso JC, Firestone J (1993) Distributions of phytoplankton blooms in the Southern Ocean. Science 262:1832–1837

Timmermans KR, van Leeuwe MA, de Jong JTM, McKay RML and 6 others (1998) Iron stress in the Pacific region of the Southern Ocean: evidence from enrichment bioassays. Mar Ecol Prog Ser 166:27–41

Treguer P, Jacques G (1992) Dynamics of nutrients and phytoplankton, and fluxes of carbon, nitrogen and silicon the Antarctic Ocean. Polar Biol 12:149–162

Trull T, Rintoul SR, Hatfield M, Abraham ER (2001) Circulation and seasonal evolution of polar waters south of Australia: implications for iron fertilization of the Southern Ocean. Deep-Sea Res II 48:2439–2466

Uno S (1982) Distribution and stocking stock of chlorophyll *a* in the Antarctic Ocean, from December 1980 to January 1981. Mem Natl Inst Polar Res (Spec Issue) 23:20–27

Uno S (1983) The relation between phytoplankton standing stock and water temperature in the Antarctic Ocean in summer, 1980–1981. Mem Natl Inst Polar Res (Spec Issue) 27:37–49

Van Leeuwe MA, Scharek R, De Baar HJW, De Jong JTM, Goeyens L (1997) Iron enrichment experiments in the Southern Ocean: physiological responses of plankton communities. Deep-Sea Res II 44(1–2):189–207

Watanabe K, Nakajima Y (1982) Vertical distribution of chlorophyll *a* along 45° E in the Southern Ocean, 1981. Mem Natl Inst Polar Res (Spec Issue) 23:73–86

Watson AJ (2001) Iron limitation in the oceans. In: Turner DR, Hunter KA (eds) The biogeochemistry of iron in seawater. John Wiley & Sons, London, p 9–39

Weber LH, El-Sayed SZ (1987) Contributions of the net, nano- and picoplankton to the phytoplankton standing crop and primary productivity in the Southern Ocean. J Plankton Res 9(5):973–994

Westerlund S, Öhman P (1991) Iron in the water column of the Weddell Sea. Mar Chem 35:199–217

Whitehouse MJ, Priddle J, Brandon MA (2000) Chlorophyll/nutrient characteristics in the water masses to the north of South Georgia, Southern Ocean. Polar Biol 23: 373–382

Yamaguchi Y, Shibata Y (1982) Stocking stock and distribution of phytoplankton chlorophyll in the Southern Ocean south of Australia. Trans Tokyo Univ Fish 5:111–128

Yamaguchi Y, Kosaki S, Aruga Y (1985) Primary productivity in the Antarctic Ocean during the austral summer of 1983/84. Trans Tokyo Univ Fish 6:67–84

Editorial responsibility: Otto Kinne (Editor-in-Chief), Oldendorf/Luhe, Germany

Submitted: September 15, 2004; Accepted: March 8, 2005
Proofs received from author(s): July 12, 2005